Pan-cancer evaluation of tumor-infiltrating lymphocytes and programmed cell death protein ligand-1 in metastatic biopsies and matched primary tumors

Zakhia El Beaino, Laëtitia Fuhrmann, Charlotte Martinat, Anne Vincent-Salomon, Célia Dupain, Grégoire Marret, Maral Halladjian, Christophe Le Tourneau, Maud Kamal, Xavier Paoletti, et al.

Journal of Pathology
J Pathol October 2024; **264:** 186–196
Published online 29 July 2024 in Wiley Online Library
(wileyonlinelibrary.com) DOI: 10.1002/path.6334

ORIGINAL ARTICLE

Pan-cancer evaluation of tumor-infiltrating lymphocytes and programmed cell death protein ligand-1 in metastatic biopsies and matched primary tumors

Zakhia El Beaino[1†], Célia Dupain[2†], Grégoire Marret[2], Xavier Paoletti[3,4], Laëtitia Fuhrmann[1], Charlotte Martinat[1], Yves Allory[5], Maral Halladjian[2], Ivan Bièche[6,7,8], Christophe Le Tourneau[2,3,9], Maud Kamal[2†] and Anne Vincent-Salomon[1*†]

[1] *Department of Pathology, Institut Curie, PSL Research University, Paris, France*
[2] *Department of Drug Development and Innovation (D3i), Institut Curie, Paris, France*
[3] *INSERM U900 Research Unit, Institut Curie, Saint-Cloud, France*
[4] *Department of Biostatistics, Institut Curie, Paris, France*
[5] *Department of Pathology, Institut Curie, Saint-Cloud, Versailles Saint-Quentin University, Paris-Saclay, France*
[6] *Department of Genetics, Institut Curie, Paris, France*
[7] *INSERM U1016 Research Unit, Paris, France*
[8] *Faculty of Pharmaceutical and Biological Sciences, Paris-Cité University, Paris, France*
[9] *Paris-Saclay University, Paris, France*

**Correspondence to: A Vincent-Salomon, Department of Pathology, Institut Curie, PSL Research University, 26 rue d'Ulm, 75005 Paris, France. E-mail: anne.salomon@curie.fr.*

[†]These authors contributed equally.

Abstract

Tumor immunological characterization includes evaluation of tumor-infiltrating lymphocytes (TILs) and programmed cell death protein ligand-1 (PD-L1) expression. This study investigated TIL distribution, its prognostic value, and PD-L1 expression in metastatic and matched primary tumors (PTs). Specimens from 550 pan-cancer patients of the SHIVA01 trial (NCT01771458) with available metastatic biopsy and 111 matched PTs were evaluated for TILs and PD-L1. Combined positive score (CPS), tumor proportion score (TPS), and immune cell (IC) score were determined. TILs and PD-L1 were assessed according to PT organ of origin, histological subtype, and metastatic biopsy site. We found that TIL distribution in metastases did not vary according to PT organ of origin, histological subtype, or metastatic biopsy site, with a median of 10% (range: 0–70). TILs were decreased in metastases compared to PT (20% [5–60] versus 10% [0–40], $p < 0.0001$). CPS varied according to histological subtype ($p = 0.02$) and biopsy site ($p < 0.02$). TPS varied according to PT organ of origin ($p = 0.003$), histological subtype ($p = 0.0004$), and metastatic biopsy site ($p = 0.00004$). TPS was higher in metastases than in PT ($p < 0.0001$). TILs in metastases did not correlate with overall survival. In conclusion, metastases harbored fewer TILs than matched PT, regardless of PT organ of origin, histological subtype, and metastatic biopsy site. PD-L1 expression increased with disease progression.

Keywords: PD-L1; tumor-infiltrating lymphocytes; metastatic biopsies; primary tumors; SHIVA01; CPS; TPS

Received 3 January 2024; Revised 22 May 2024; Accepted 19 June 2024

No conflicts of interest were declared.

Introduction

Tumors can escape immunosurveillance by increasing signaling through co-inhibitory receptors or immune checkpoint proteins on T cells. These include programmed cell death protein-1 (PD-1) and cytotoxic T-lymphocyte antigen-4 (CTLA-4) [1]. Immune checkpoint inhibitors (ICIs), such as CTLA-4, PD-1, and programmed cell death protein ligand-1 (PD-L1) inhibitors, have positively impacted cancer treatment and improved patient survival in different cancer types [2–5].

PD-L1 expression assessed by immunohistochemistry (IHC) was one of the first biomarkers to be used in routine clinical practice for ICI treatment [6]. Several scoring systems evaluating various tumor and immunological cellular compartments have been developed for quantifying PD-L1 expression, including the tumor proportion score (TPS) [7], the combined positive score (CPS) [8], and the immune cell (IC) score [9]. Meanwhile, specific

recommendations for PD-L1 evaluation have been defined according to the different tumor types based on the organ of origin [10]. Further research is under way focusing on the development of algorithms and artificial intelligence to be proficiently incorporated into daily diagnostic workflow so as to assist pathologists in routinely scoring PD-L1 according to cancer type [11,12].

While the US Food and Drug Administration (FDA) has approved several companion IHC assays for PD-L1 depending on the type of ICI, PD-L1 IHC 22C3 pharmDx is currently the most widely used for many tumor types [10]. PD-L1 IHC expression has become a selection criterion for some ICIs, such as pembrolizumab. PD-L1 IHC status is today a predictive biomarker, for which evidence and protocols are already available for many tumors [10]. Nevertheless, PD-L1 remains an imperfect biomarker, as responses to ICIs are also observed in PD-L1-low or -negative patients. On the other hand, the assessment of immune infiltrate in tumors, most commonly referred to as tumor-infiltrating lymphocytes (TILs), is gaining importance in the current quest for optimal biomarkers to select patients with the highest likelihood of responding to immunotherapeutic agents [13]. TIL assessment has more recently been suggested as a biomarker to be included in routine histopathology reporting [14,15]. Thus, immunological categorizations of tumors and their microenvironments based on combined PD-L1 expression and TIL determination have been proposed [16,17].

Other biomarkers of ICI efficacy have been identified, namely microsatellite instability (MSI) [18,19], which is caused by defects in mismatch repair genes (*MSH2*, *MLH1*, *MSH6*, or *PMS2*) and leads to increased mismatch errors [20–22]. *POLE* pathogenic mutations resulting in ultramutated genomes were also shown to predict response to ICIs [1,18,19]. Finally, tumor mutational burden (TMB), defined as the total number of nucleotide variants per megabase (Mb), was shown to be correlated with pembrolizumab efficacy [23]. However, MSI and *POLE*-mutated tumors remain rare, and the lack of harmonized methods for calculating TMB and robust cut-offs limits its use as a biomarker in clinical practice.

The immunological microenvironment exhibits variations in histological subtypes of cancers from the same primary organ (organ of origin), e.g. in gastric cancer, with different immune contextures and PD-L1 expression patterns described according to the tumor subtypes [24].

These immunological variations are currently described in primary tumors (PTs), but to our knowledge, sufficient data are still lacking in the literature regarding the evaluation of the immunological microenvironment in pan-cancer metastatic tumors of different histologies [13,25–27].

Based on these observations, the objectives of this study were as follows: (1) to describe the distribution of TILs and PD-L1 in metastatic samples across different organs of origin and histological subtypes, (2) to compare TIL distribution and PD-L1 expression in matched primary and metastatic tumors, and (3) to correlate TILs with patient outcomes. To this end, matched pan-cancer metastatic and primary solid tumors from patients included in the SHIVA01 trial (NCT01771458) were used for a combined evaluation of TILs and PD-L1 by IHC.

Materials and methods

Patient selection

Samples of 550 patients from the SHIVA01 clinical trial (NCT01771458) were used for this study [28,29]. All patients were included after written informed consent was obtained.

In addition, we collected 111 samples of PT matched with the respective metastatic samples from SHIVA01 (Figure 1). Matched PT samples were whole-tissue samples from surgical resection specimens ($n = 95/111$; 86%) and biopsies ($n = 16/111$; 14%).

Hematoxylin and eosin-stained (HES) slides and TIL evaluation

All 550 metastatic patient samples were centralized at the Institut Curie, Paris, France, as part of the SHIVA01 trial and preserved under optimal tissue banking conditions.

Stromal TILs were reported as a percentage according to the recommendations of the International TILs Working Group [30] (see Supplementary materials and methods).

The 111 matched PT samples were assessed in the same manner.

IHC and PD-L1 evaluation

IHC staining was carried out on 4-µm-thick sections using an Autostainer Plus (Agilent Technologies, Inc., Santa Clara, CA, USA) with appropriate positive controls (Supplementary materials and methods).

For the CPS, clinically relevant cut-offs of 0, ≥1–<10, ≥10–<20, and ≥20 were used [10,31,32]. For the TPS, three cut-offs of 0, ≥1, and ≥50 were used [10,31,33]. No cut-off was used for the IC score.

Statistics

All statistical tests used for TIL and PD-L1 comparative studies are detailed in Supplementary materials and methods.

Correlations with patient outcome

Overall survival (OS) outcomes were recorded for 513/550 patients. OS was measured from the date of entry into the trial until death. OS was estimated using the Kaplan–Meier method. Participants without any event were censored for survival analyses.

Organ of origin of primary tumor	Median no. TILs [0–70]
Breast (*n* = 73)	**10% [0–70]**
Gastrointestinal (*n* = 145)	**10% [0–45]**
Colorectal (*n* = 59)	10% [0–40]
Pancreatic adenocarcinoma (*n* = 38)	10% [0–25]
HCC (*n* = 17)	10% [2–20]
Oesogastric adenocarcinoma (*n* = 16)	10% [1–45]
Anal SCC (*n* = 8)	5% [1–15]
Oesogastric SCC (*n* = 4)	13% [1–25]
Neuroendocrine tumor (*n* = 3)	5% [2–10]
Skin (*n* = 10)	**10% [1–25]**
Melanoma (*n* = 6)	10% [1–25]
Merkel cell carcinoma (*n* = 2)	10% [10–10]
SCC (*n* = 1)	10%
Trichoblastic carcinoma (*n* = 1)	5%
Soft Tissue Sarcoma (*n* = 32)	**10% [0–35]**
Other (*n* = 4)	**7.5% [5–20]**
Peritoneum (*n* = 1)	5%
Neuroendocrine tumor (*n* = 1)	5%
Meningioma (*n* = 1)	10%
Myxopapillary ependymoma (*n* = 1)	20%
CUP (*n* = 19)	**10% [5–50]**

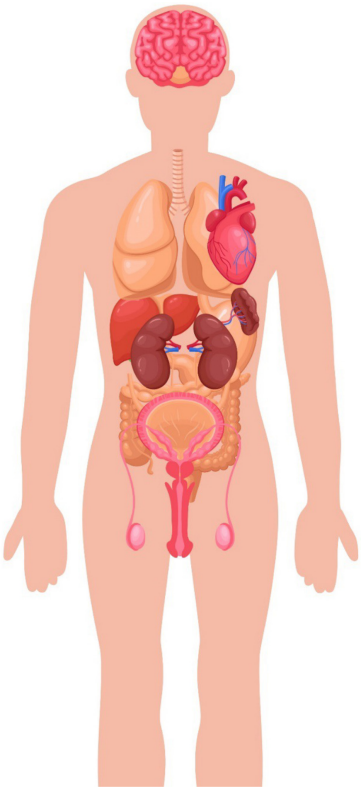

Organ of origin of primary tumor	Median no. TILs [0–70]
Eye (*n* = 8)	**10% [2–25]**
Uveal melanoma (*n* = 7)	10% [2–10]
Ocular adenocarcinoma (*n* = 1)	25%
Head & Neck (*n* = 51)	**10% [0–30]**
HNSCC (*n* = 23)	10% [2–30]
Salivary gland tumor (*n* = 20)	10% [0–15]
Thyroid (*n* = 4)	10% [0–15]
UCNT (*n* = 4)	10% [5–30]
Thoracic (*n* = 78)	**10% [0–60]**
Lung (*n* = 72)	10% [0–60]
Pleura (*n* = 3)	10%
Thymus (*n* = 2)	6% [1–10]
Mediastinum (*n* = 1)	15%
Genitourinary (*n* = 29)	**10% [1–35]**
Urothelial (*n* = 19)	10% [1–35]
Kidney cancer (*n* = 6)	10% [2–15]
Penile SCC (*n* = 2)	7.5% [5–10]
Adrenocortical carcinoma (*n* = 1)	25%
Prostate adenocarcinoma (*n* = 1)	10 %
Gynecology (*n* = 101)	**10% [0–60]**
Ovary (*n* = 58)	10% [0–60]
Cervix (*n* = 22)	10% [1–35]
Uterus (*n* = 19)	10% [0–30]
Pelvis (*n* = 1)	10 %
Vulva (*n* = 1)	10 %

Figure 1. Median distribution of TILs in metastases according to primary tumor organ of origin. Maximum and minimum ranges are given as percentage indicated in brackets. Royalty-free image taken from the PNGTree website. CUP, cancer of unknown primary origin; HCC, hepatocellular carcinoma; HNSCC, head and neck squamous cell carcinoma; SCC, squamous cell carcinoma; UCNT, undifferentiated carcinoma of the nasopharyngeal type. Image figure created with BioRender.com

Multivariate analyses and univariate hazard ratios (HRs) for comparisons of covariates were generated by Cox proportional hazards regression analysis.

TILs were measured as a percentage and then converted to a categorical variable, i.e. TILs <10% and TILs ≥10%.

Median follow-up was estimated using the reverse Kaplan–Meier method for censored times. Survival curves were generated using Kaplan–Meier estimates and compared with the log-rank test. Qualitative changes between matched PT and metastases in TILs and IC score were characterized, and related subgroups were compared for survival. All tests were two-sided, with the level of significance set at $p < 0.05$.

Results

Patient characteristics

TIL assessment was available for 550 metastatic biopsies (100%) and 111 matched PT (20%). Overall, 494 out of 550 metastatic tumors (90%) and 77 matched PTs (16%) were evaluated for PD-L1 by IHC (supplementary material, Figure S1). The main PT organs of origin and histological types are summarized in Figure 1 and supplementary material, Table S1.

Metastatic tumors in different anatomical sites were subdivided into six groups (supplementary material, Figure S2), including liver biopsies (TILs: $n = 179/550$; 33%; PD-L1: $n = 162/494$; 33%), lung biopsies (TILs: $n = 96/550$; 18%; PD-L1: $n = 84/494$; 17%), lymph node biopsies (TILs: $n = 88/550$; 16%; PD-L1: $n = 78/494$; 16%), cutaneous biopsies (TILs: $n = 53/550$; 9.6%; PD-L1: $n = 49/494$; 10%), other biopsies (TILs: $n = 133/550$; 24%; PD-L1: $n = 120/494$; 24%), and brain biopsy (TILs: $n = 1/550$; 0.2%; PD-L1: $n = 1/494$; 0.2%) (supplementary material, Table S1).

Evaluation of TILs in metastatic biopsies

Median TIL proportion in metastatic biopsies was 10% (range: 0–70) (Figure 1). Distribution of TILs according to PT organs of origin, histological types, and metastatic biopsy sites is summarized in Figure 2. There was no significant association between TILs and the PT organs of origin ($p = 0.6$), histological types ($p = 0.8$), and metastatic biopsy sites ($p = 0.07$).

Evaluation of TILs in matched primary and metastatic tumors

Mean TIL proportion was significantly higher in PTs than in matched metastases (mean [range]: 20.8% [18.7–22.9%] versus 11.6% [9.9–13.4%]; $p < 0.0001$) (Figures 3 and 4A). When focusing on the PT organs of origin, mean TIL proportion in primary breast and gynecological tumors was significantly higher than in

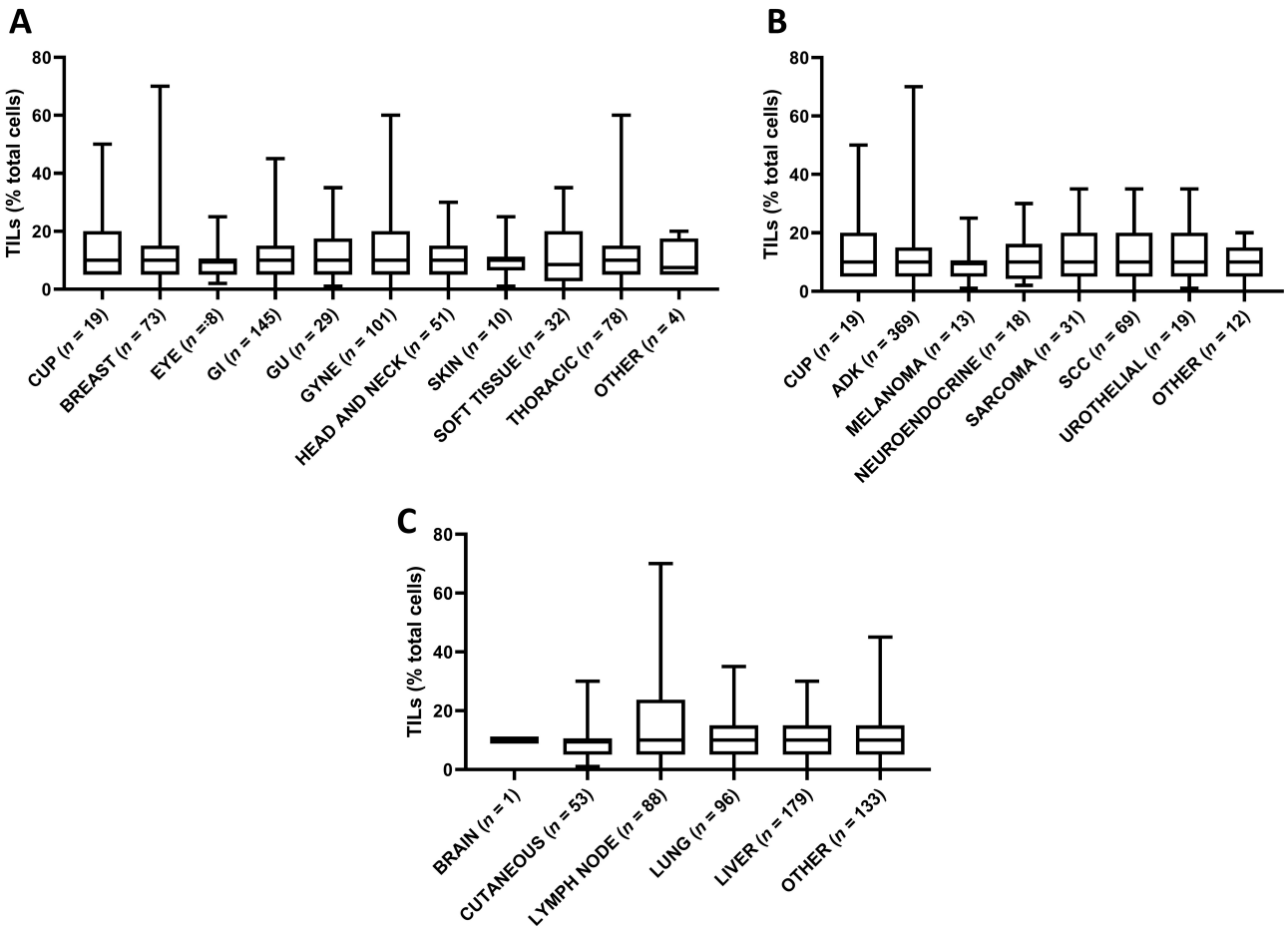

Figure 2. Distribution of TILs in metastases by (A) organ of origin, (B) histological type, and (C) metastatic biopsy site. Data are presented as continuous variables (box and whisker plots, with bars corresponding to min and max values). A Kruskal–Wallis test followed by Dunn's test was used to compare the percentage of TILs within each group. No significant difference was found. ADK, adenocarcinoma; CUP, cancer of unknown primary origin; GI, gastrointestinal; GU, genitourinary; GYNE, gynecological; SCC, squamous cell carcinoma; TIL, tumor-infiltrating lymphocyte.

matched metastases (20% [5–40%] versus 10% [0–25%]; $p < 0.001$) (Figure 3B). Regarding histological types, mean TIL proportion in adenocarcinoma (ADK) was significantly higher in PTs than in matched metastases (19.9% [5–45%] versus 9.8% [1–40%]; $p < 0.0001$) (Figure 3C). According to the different metastatic biopsy sites, there was no significant difference in mean TIL proportion between PT and matched metastases (Figure 3D).

Evaluation of PD-L1 expression in metastatic biopsies

The CPS, TPS, and IC score of PD-L1 expression were assessed either as continuous variables or as cut-off categories, according to PT organs of origin, histological types, and metastatic biopsy sites (Figure 4 and supplementary material, Figures S3–S5).

Positive PD-L1 expression (i.e. CPS >0) was found in 321 out of 494 patients (65%). CPS 0, ≥1–<10, ≥10–<20, and ≥20 were observed in 173 (35%), 180 (36%), 39 (8%), and 102 patients (21%), respectively (supplementary material, Table S2).

Based on guidelines and recent literature on PD-L1 expression, PD-L1 expression was assessed using a CPS cut-off of ≥10, thus encompassing all possible situations and indications [10,27].

A CPS ≥10 was found in breast ($n = 19/60$; 32%), genitourinary (GU) ($n = 8/29$; 28%), eye ($n = 3/7$; 43%), carcinoma of unknown primary origin (CUP) ($n = 8/19$; 42%), head and neck ($n = 19/43$; 44%), gynecological (GYNE) ($n = 34/93$; 37%), thoracic ($n = 22/69$; 32%), gastrointestinal (GI) ($n = 25/131$; 19%), and soft-tissue ($n = 3/29$; 10%) cancers (Figure 4A and supplementary material, Table S2). A significant association was observed between organs of origin and a CPS ≥10 or <10 ($p = 0.002$).

A CPS ≥10 was found in metastases arising from squamous cell carcinoma (SCC) ($n = 31/66$; 47%), CUP ($n = 8/19$; 42%), other histological types ($n = 4/11$; 36%), urothelial ($n = 6/19$; 32%), neuroendocrine ($n = 5/17$; 29%), melanoma ($n = 3/12$; 25%), ADK ($n = 82/322$; 26%), and sarcoma histological types ($n = 2/28$; 7%) (Figure 4B and supplementary material, Table S2). A significant association was observed between histological types and a CPS ≥10 or <10 ($p = 0.003$).

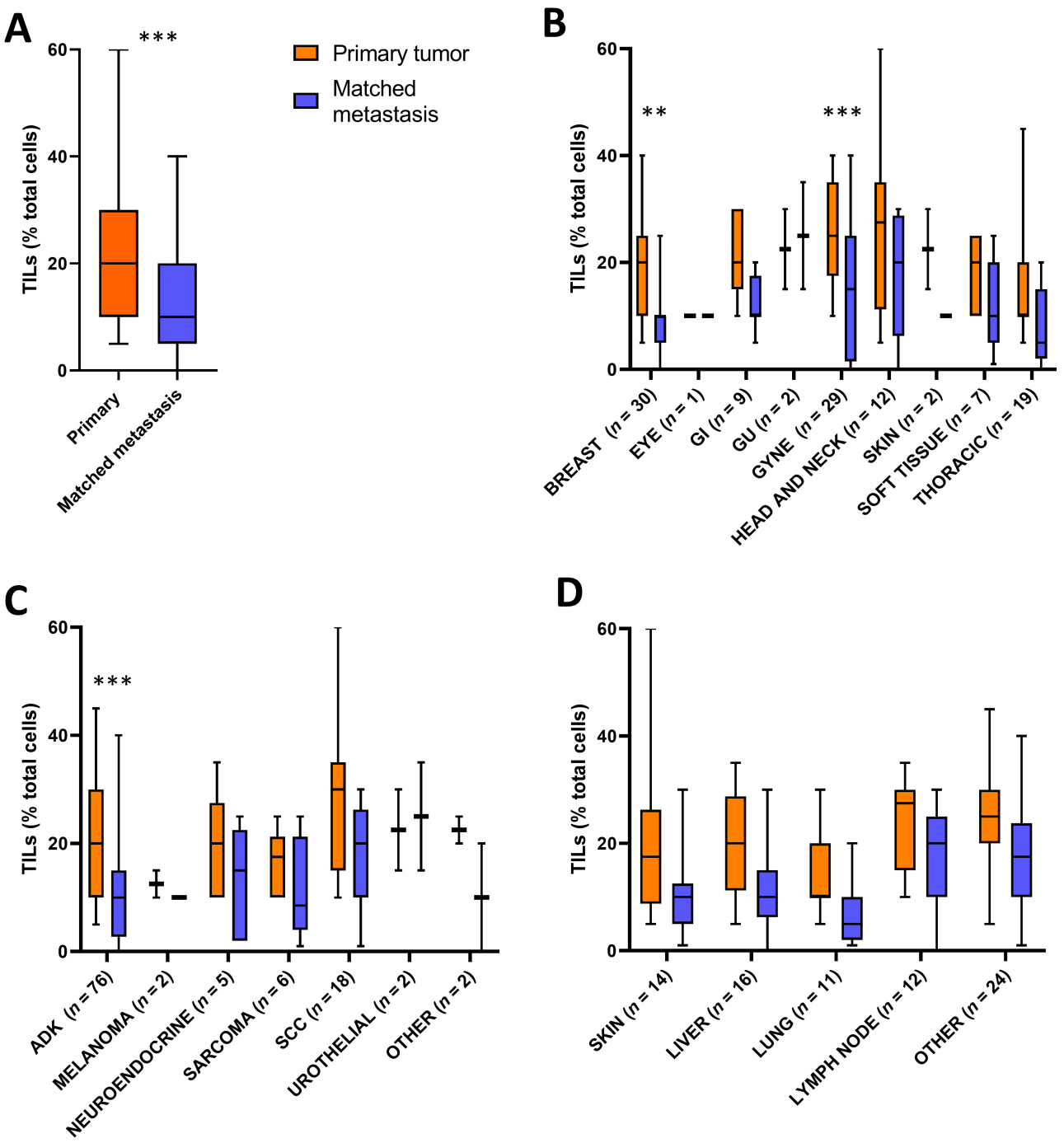

Figure 3. Comparison of TIL distribution (A) in all matched primary and metastatic tumors and by (B) organ of origin, (C) histological subtype, and (D) metastatic biopsy site of metastasis. Data are presented as continuous variables (box and whisker plots, bars corresponding to min and max values). Paired *t*-tests were used to compare percentage of TILs within primary tumors and metastases. Multiple *t*-test was used to compare percentage of TILs within primary tumors and metastases and according to the different groups. $^{**}p < 0.001$; $^{***}p < 0.0001$. ADK, adenocarcinoma; GI, gastrointestinal; GU, genitourinary; GYNE, gynecological; SCC, squamous cell carcinoma; TIL, tumor-infiltrating lymphocyte.

A CPS ≥10 was found in metastases arising from skin biopsies ($n = 16/49$; 33%), lymph node biopsies ($n = 36/78$; 46%), other biopsies ($n = 31/120$; 26%), liver biopsies ($n = 39/162$; 24%), and lung biopsies ($n = 19/84$; 23%) (Figure 4C and supplementary material, Table S2). A significant association was observed between metastatic biopsy sites and a CPS ≥10 or <10 ($p = 0.003$).

Using clinically relevant cut-offs in head and neck SCC, CPS ≥1 and CPS ≥20 were found in 15 and 14 out of 43 head and neck metastases, respectively (35 and 33%, respectively) (Figure 4A and supplementary material, Table S2).

TPS ≥ 1% and TPS ≥ 50% were analyzed in CUP ($n = 12/19$; 63% versus $n = 0/19$; 0%), breast ($n = 29/60$; 48.3% versus $n = 3/60$; 5%),

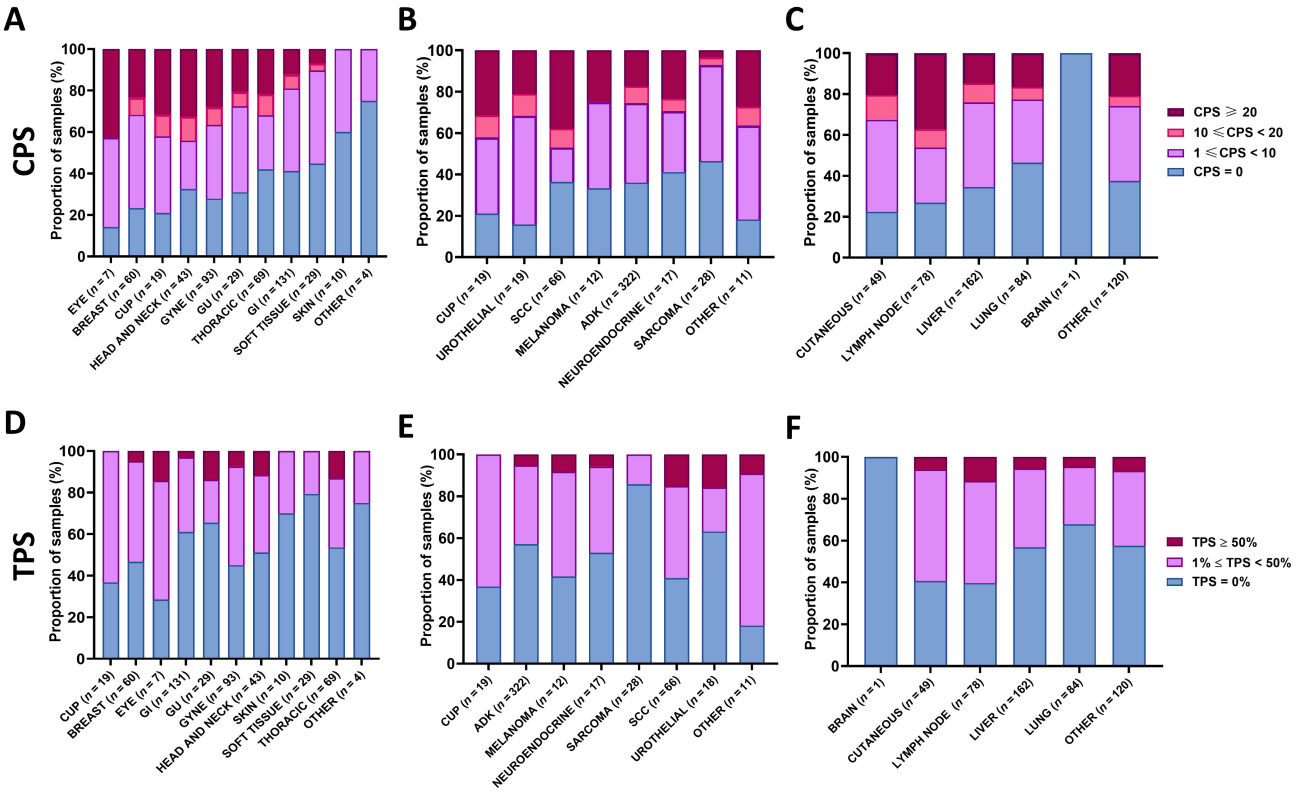

Figure 4. Distribution of PD-L1 expression in metastases based on CPS by (A) organ of origin, (B) histological type, and (C) metastatic biopsy site and based on TPS by (D) organ of origin, (E) histological type, and (F) metastatic biopsy site. PD-L1 expression is represented by the combined positive score (CPS). Data are presented as proportion of samples. Distribution of CPS classes by organ of origin: $p = 0.02$; distribution of CPS classes by histological type: $p = 0.02$; distribution of CPS classes by biopsy site: $p = 0.002$. Distribution of TPS classes by organ of origin: $p = 0.003$; distribution of TPS classes by histological type: $p = 0.0004$; distribution of TPS classes by biopsy sites: $p = 0.01$. ADK, adenocarcinoma; CNS, central nervous system; CPS, combined positive score; CUP, cancer of unknown primary origin; GI, gastrointestinal; GU, genitourinary; GYNE, gynecological; SCC, squamous cell carcinoma; TPS, tumor proportion score.

GYNE ($n = 44/93$; 47.3% versus $n = 70/93$; 75%), and thoracic tumors ($n = 23/69$; 33.3% versus $n = 9/69$; 13%) (Figure 4D). A significant association was found between organs of origin and a TPS ≥1% or ≥50% ($p = 0.003$, Figure 4D).

The proportions of samples with a TPS ≥1% and ≥50% were highest in SCC ($n = 29/66$; 43.9% and $n = 10/66$; 15.2%, respectively) and ADK ($n = 121/322$; 37.6% and $n = 17/322$; 5.3%). There was an association between the histological subtypes and a TPS ≥1% or ≥50% ($p = 0.0004$) (Figure 4E).

The proportions of samples with a TPS ≥1% and ≥50% were highest in skin biopsies ($n = 26/49$; 53.1% and $n = 3/49$; 6.1%, respectively) and lymph node biopsies ($n = 38/78$; 48.7% and $n = 9/78$; 11.5%). There was an association between metastatic biopsy sites and a TPS ≥1% or ≥50% ($p = 0.01$) (Figure 4F).

The use of PD-L1 expression scoring systems as continuous variables revealed significant differences for CPS between organs of origin ($p = 0.001$) and biopsy sites ($p = 0.004$), for TPS between organs of origin ($p = 0.005$), histological types ($p = 0.0003$), and biopsy sites ($p = 0.001$), and for IC score between organs of origin ($p < 0.001$) and biopsy sites ($p = 0.003$) (supplementary material, Figures S3–S5).

All results for TIL and PD-L1 evaluations in metastases are detailed in supplementary material, Table S1.

There was a moderate, albeit significant, correlation between TIL proportions and CPS and TPS (Pearson correlation $r = 0.32$, $p < 0.001$ and $r = 0.3$, $p < 0.001$, respectively).

Evaluation of PD-L1 expression in matched primary and metastatic tumors

Mean TPS was significantly lower in PTs than in matched metastases (13% [0–90%] versus 20% [0–95%]; $p = 0.007$; Figure 5B and supplementary material, Table S3), whereas no differences were observed with regard to mean CPS ($p = 0.9$) and IC score ($p = 0.9$) (Figure 5A,C). There were no significant differences between matched PTs and metastatic tumors with regard to CPS subgroups according to 1, 10, and 20% cut-offs (Figure 5A) or TPS ≥1% and ≥50% (Figure 5B).

No differences in TILs, TPS, CPS, and IC score across organs of origin, histological types, or biopsy sites were observed in matched PTs and metastatic tumors (supplementary material, Figures S6–S10 and Table S3).

All results for TIL and PD-L1 evaluations in matched metastases are detailed in supplementary material, Table S4.

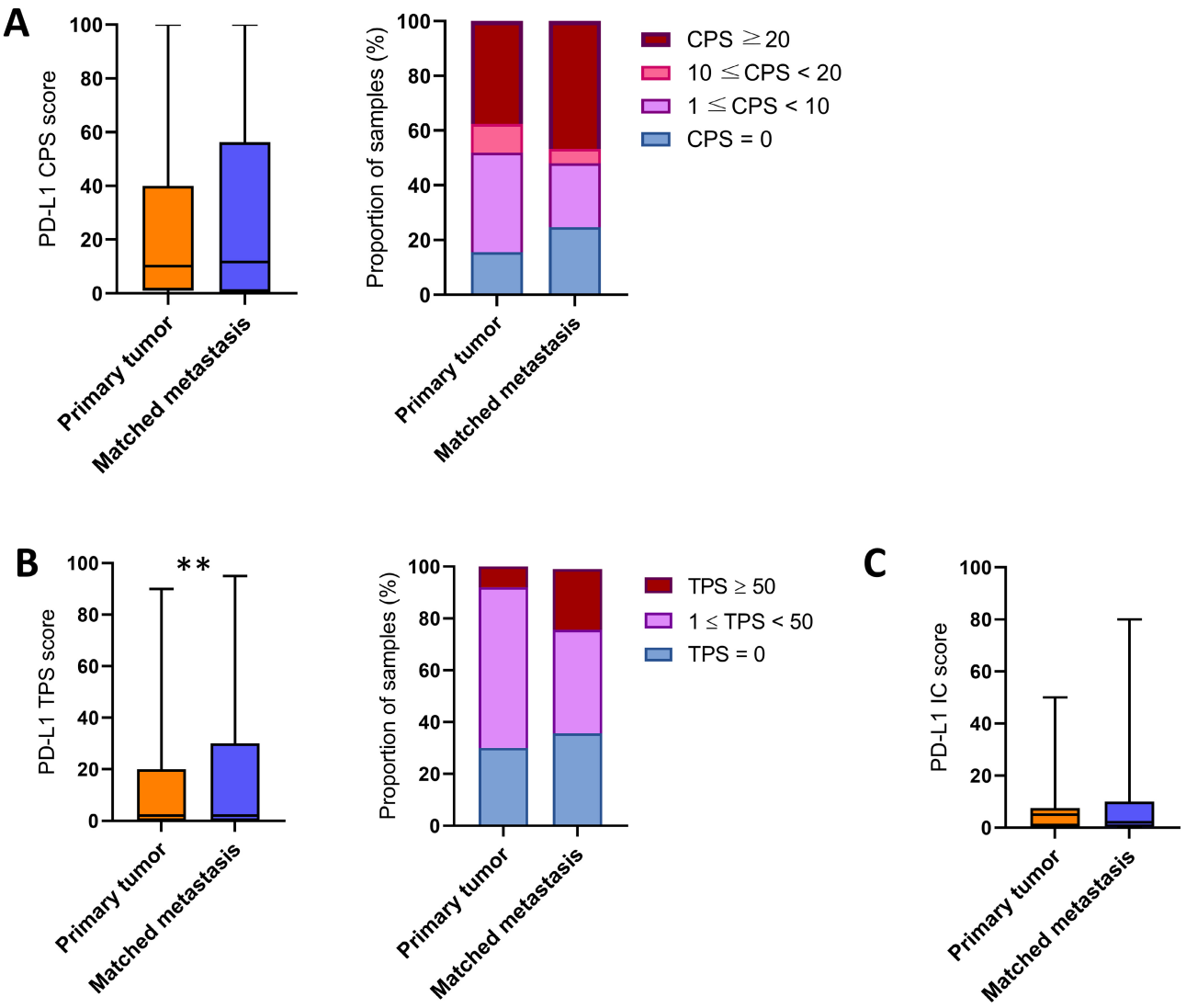

Figure 5. Comparison of PD-L1 expression distribution in matched primary and metastatic tumors according to (A) CPS, (B) TPS, and (C) IC score. Data from the left panels are presented as continuous variables (box and whisker plots, bars corresponding to min and max values), while data from the right panels are presented as proportion of samples. For continuous variables, paired *t*-test was used to compare PD-L1 expression within primary and metastasis tumors. $^{**}p < 0.001$. To compare proportions of samples between primary tumors and metastases, McNemar's chi-squared test was used (CPS: $p = 0.9$ and TPS: $p = 0.5$). CPS, combined positive score; IC score, immune cells positive for PD-L1 immunostaining; PD-L1, programmed cell death protein ligand-1; TPS, tumor proportion score.

Prognostic value of TILs

Survival curves by organ of origin, histological type, and metastatic biopsy site are shown in supplementary material, Figure S11A–C. Organs of origin and histological types were found to be prognostic factors of OS in univariate analyses ($p < 0.001$). Survival curves for OS according to TILs ≥10% are presented in supplementary material, Figures S12–S15. In univariate analyses, TILs ≥10% had no prognostic significance either in the whole patient cohort ($p = 0.7$) or according to organ of origin, histological subtype, and metastatic biopsy site.

Discussion

To our knowledge, this study is the first to analyze TIL distribution and PD-L1 expression in specimens of pan-cancer metastatic tumors previously treated with systemic therapy and compare them with matched PT.

In our study, a homogeneous distribution of TIL proportions in metastases was observed irrespective of the PT organ of origin, histological type, and metastatic biopsy site. The immune signature seems to be a stable phenotypic marker for the disease and is remarkably reproduced across all metastatic sites, histological types, and organs of origin.

This observation could reflect either a potential 'imprinting' of the immune microenvironment by the tumor cells or the possibility that the immune contexture in PTs results in 'educated' ICs that are recalled in the different metastatic sites [34,35].

Interestingly, we found that metastatic tumors had a significantly lower percentage of TILs compared to their matched PTs ($p < 0.0001$). Such significantly decreased

lymphocytic infiltrate was observed across all histological types and organs of origin.

Our study shows a general trend of increased TILs in PTs than in matched metastases although not significant for all tumor types and histologies. Our limited number of cases per tumor type might not capture all histology-specific nuances, as highlighted by Loi *et al* for breast cancer metastases. A larger dataset will be required to clearly assess the distinct patterns of TILs across various cancer types [36].

The difference in immune microenvironment between primary and metastatic lesions suggests a tumor adaptation as it progresses from early to advanced disease. These differences are likely to be dynamic and sensitive to intrinsic (e.g. mutations and cell–cell communication) and extrinsic perturbations such as treatment modalities [37–39].

Our study is consistent with numerous data in the literature regarding PD-L1 expression assessed by CPS or TPS in the different organs of origin. For example, positive CPS PD-L1 expression (CPS ≥ 10%) in breast cancer was 31.7% in our study, as compared to 38% in the literature [40]. In lung cancer, we found positive PD-L1 expression levels using cut-off values of 1% ≤ TPS ≤ 49% and TPS ≥ 50% of 33.3 and 13%, as compared to 37.03% [41] and 13.29% [41] in the literature, respectively. As for head and neck cancers, PD-L1 positivity (CPS≥1%) has been reported in 85% of patients in the KEYNOTE-048 study [31], compared to 67% in our metastatic head and neck cohort. This difference could be explained by the use of archival and newly collected biopsies in the KEYNOTE-048 study, while our assessment was on metastatic biopsies only.

Generally, lower levels of TILs have been associated with lower CPS, acknowledging TILs as a component of the CPS evaluation [42]. This correlation highlights the integrated role TILs play in immunotherapeutic responsiveness and prognostic assessment. TIL proportions and PD-L1 expression do not have a strong correlation, although it is significant in our dataset. This relationship can vary with tumor histology, affecting the CPS/TPS and treatment decisions. Our findings indicate that this relationship is not uniformly linear across different tumor types or between histologies such as ADK and SCC, which could be attributed to the differential regulation of PD-L1 in these cancers. Our results underscore the need for a nuanced interpretation of CPS/TPS, taking into account the histology-specific PD-L1 regulation and the interplay with TILs, which could ultimately refine patient selection for checkpoint inhibitor therapies.

In our study, we found a significant variation when comparing PD-L1 expression in metastases using the CPS and TPS according to the organ of origin, histological subtype, and metastatic biopsy site. This is consistent with many findings in the literature regarding oncogene-driven PD-L1 expression issues [6]. Numerous cell signaling perturbations have been associated with constitutive PD-L1 expression across organs of origin and histological subtypes. For example, *PTEN* loss has been associated with upregulated PD-L1 in glioblastoma multiforme and colorectal cancer [43,44].

The significant variation in PD-L1 expression according to metastatic biopsy site is also a major finding of our study because of the limited data in the literature comparing pan-cancer PD-L1 status. The significant variation in oncogene-mediated PD-L1 expression by biopsy site is consistent with the hypothesis of a local interferon (IFN)-γ-induced PD-L1 expression, a dynamic biomarker present at sites of active inflammation [45]. Thus, biopsy samples represent a snapshot of the tumor immune microenvironment in space [46].

In matched tumors, comparisons of PD-L1 expression using the CPS, TPS, and IC score in the different organs of origin, histological subtypes, and metastatic biopsy sites did not reach statistical significance, though with a slight trend toward increased expression in metastases compared to PT. This could be explained by our heavily pretreated population in the metastatic setting and the small size of metastatic biopsies, which prevented the assessment of the entire tumor surface.

Interestingly, metastatic tumors had a higher mean TPS than matched PTs ($p < 0.001$), which may be caused by the immune evasion and modulation of the microenvironment by the increased inflammatory cytokines, particularly IFN-γ, released by TILs, even if present at low density, in metastases. This would induce PD-L1 upregulation in tumors as an adaptive immune resistance mechanism to suppress local effector T-cell function against autoimmune attack [46,47]. This heterogeneity in PD-L1 expression was in line with the results of Wang *et al* in 22 patients with metastatic colorectal cancer whose metastatic lesion showed higher PD-L1 expression than the primary tumor [48]. Meanwhile, similar results were obtained for non-small cell lung cancer, endometrial cancer, and breast cancer, for example [49–51].

Overall, the clinical outcome was not significantly correlated with the percentage of TILs, which could be accounted for by the limited number of PTs evaluated or the heterogeneity of our pan-cancer cohort. Different tumor and histological types were actually evaluated. In addition, the SHIVA01 patients had received various treatments in view of their advanced stage disease.

In considering the broader implications of our findings within the Companion Diagnostic (CdX) narrative, particularly as critiqued in *The Lancet Oncology* [52], it is apparent that our study offers tangible evidence to advance the discourse. The industry-driven narrative commonly promotes distinct CdX for individual histologies. In contrast, our pan-cancer analysis underscores the complexity of PD-L1 expression and TILs across cancers, suggesting that the development of CdX should not be constrained to a uniform approach but rather should be adaptive to the variegated landscape of tumor immunobiology. Our results advocate for a multifaceted CdX model, responsive to the intricate immune profiles exhibited by different tumor types and their metastatic counterparts. Aligning with the solutions proposed by the authors in *The Lancet Oncology*, we support a concerted move toward a CdX framework that is both fluid

and reflective of diverse patient needs, underscored by rigorous scientific substantiation. Such an approach ensures that the trajectory of CdX development remains steadfastly patient-centric and scientifically grounded and taking into account as far as possible worldwide economic sustainability. Considering all the evidence, TILs can therefore be used to evaluate the quality of the PDL1-stain; for example, the PDL1-stain is probably false-negative if the HES slide shows many TILs.

Our study had the limitations inherent in retrospective studies. First, all metastatic samples were biopsies instead of whole-tissue specimens, thereby limiting microenvironment evaluation and preventing us from assessing geometrical expression and variation in PD-L1 in metastases. Second, the patients who were recruited in this study were treated with chemo-radiotherapy and not with immunotherapy.

Therefore, further analyses are required to evaluate the predictive value of PD-L1 and TILs for immunotherapy in the metastatic setting.

In conclusion, metastases harbored fewer TILs than matched PTs, regardless of the PT organ of origin, histological subtype, and metastatic biopsy site. The decreased TILs in metastases of matched lesions may suggest tumor adaptation in metastases, with progression from early to advanced disease. PD-L1 increased with disease progression. TILs did not have a prognostic value in metastatic samples. Molecular characterization and immunological profiling will be needed to confirm the proposed hypotheses.

Acknowledgements

We would like to thank the PATHEX team (Gabriel Champenois, André Nicolas) and the pathology department technicians of the Institut Curie (Laure Annette, Martial Kaly) for technical support in IHC staining, as well as the clinical trial investigators (Jean-Pierre Delord, Anthony Gonçalves, Céline Gavoille, Coraline Dubot, Nicolas Isambert, Mario Campone, Olivier Trédan, Marie-Ange Massiani, Cécile Mauborgne, Sebastien Armanet, Nicolas Servant, Ivan Bièche, Virginie Bernard, David Gentien, Pascal Jezequel, Valéry Attignon, Sandrine Boyault, Vincent Servois, Marie-Paule Sablin). This work was supported in part by the Department of Diagnostic and Theranostic Medicine, Institut Curie Hospital Group, Paris, France, and the Department of Drug Development and Innovation of the Institut Curie (D3i). The SHIVA01 trial was supported by grant ANR-10-EQPX-03 from the Agence Nationale de la Recherche (Investissements d'avenir) and Site de Recherche Intégré contre le Cancer (SiRIC).

Author contributions statement

Data curation was performed by ZEB, CD, LF and CM. Formal analysis by ZEB, CD, GM and XP. Original draft writing was done by ZEB, CD, MK, GM, MH, CLT and AVS. Writing and editing were done by all authors. Methodology was established by ZEB, CD, GM, XP, MK and AVS. Conceptualization and validation of the study were done by ZEB, CD, XP, YA, CLT, MK and AVS. Validation of the study was done by GM, XP, YA, IB, CLT, MK and AVS. All authors approved the final version of the manuscript.

Data availability statement

The data that support the findings of this study are available from the corresponding author upon reasonable request.

References

1. Havel JJ, Chowell D, Chan TA. The evolving landscape of biomarkers for checkpoint inhibitor immunotherapy. *Nat Rev Cancer* 2019; **19:** 133–150.
2. Baraibar I, Melero I, Ponz-Sarvise M, *et al*. Safety and tolerability of immune checkpoint inhibitors (PD-1 and PD-L1) in cancer. *Drug Saf* 2019; **42:** 281–294.
3. Shin DS, Ribas A. The evolution of checkpoint blockade as a cancer therapy: what's here, what's next? *Curr Opin Immunol* 2015; **33:** 23–35.
4. Taghizadeh H, Marhold M, Tomasich E, *et al*. Immune checkpoint inhibitors in mCRPC – rationales, challenges and perspectives. *Oncoimmunology* 2019; **8:** e1644109.
5. Edwards SC, Hoevenaar WHM, Coffelt SB. Emerging immunotherapies for metastasis. *Br J Cancer* 2021; **124:** 37–48.
6. Patel SP, Kurzrock R. PD-L1 expression as a predictive biomarker in cancer immunotherapy. *Mol Cancer Ther* 2015; **14:** 847–856.
7. Kerr KM, Tsao M-S, Nicholson AG, *et al*. Programmed death-ligand 1 immunohistochemistry in lung cancer: in what state is this art? *J Thorac Oncol* 2015; **10:** 985–989.
8. Kulangara K, Zhang N, Corigliano E, *et al*. Clinical utility of the combined positive score for programmed death Ligand-1 expression and the approval of pembrolizumab for treatment of gastric cancer. *Arch Pathol Lab Med* 2019; **143:** 330–337.
9. Vennapusa B, Baker B, Kowanetz M, *et al*. Development of a PD-L1 complementary diagnostic immunohistochemistry assay (SP142) for atezolizumab. *Appl Immunohistochem Mol Morphol* 2019; **27:** 92–100.
10. Marletta S, Fusco N, Munari E, *et al*. Atlas of PD-L1 for pathologists: indications, scores, diagnostic platforms and reporting systems. *J Pers Med* 2022; **12:** 1073.
11. Huang Z, Chen L, Lv L, *et al*. A new AI-assisted scoring system for PD-L1 expression in NSCLC. *Comput Methods Programs Biomed* 2022; **221:** 106829.
12. Inge LJ, Dennis E. Development and applications of computer image analysis algorithms for scoring of PD-L1 immunohistochemistry. *Immunooncol Technol.* 2020; **6:** 2–8.
13. Lu S, Stein JE, Rimm DL, *et al*. Comparison of biomarker modalities for predicting response to PD-1/PD-L1 checkpoint blockade: a systematic review and meta-analysis. *JAMA Oncol.* 2019; **5:** 1195–1204.
14. Galon J, Mlecnik B, Bindea G, *et al*. Towards the introduction of the 'immunoscore' in the classification of malignant tumours. *J Pathol* 2014; **232:** 199–209.

15. Donnem T, Kilvaer TK, Andersen S, *et al*. Strategies for clinical implementation of TNM-Immunoscore in resected nonsmall-cell lung cancer. *Ann Oncol.* 2016; **27:** 225–232.
16. Vilain RE, Menzies AM, Wilmott JS, *et al*. Dynamic changes in PD-L1 expression and immune infiltrates early during treatment predict response to PD-1 blockade in melanoma. *Clin Cancer Res.* 2017; **23:** 5024–5033.
17. Teng MWL, Ngiow SF, Ribas A, *et al*. Classifying cancers based on T-cell infiltration and PD-L1. *Cancer Res* 2015; **75:** 2139–2145.
18. Overman MJ, McDermott R, Leach JL, *et al*. Nivolumab in patients with metastatic DNA mismatch repair-deficient or microsatellite instability-high colorectal cancer (CheckMate 142): an open-label, multicentre, phase 2 study. *Lancet Oncol* 2017; **18:** 1182–1191.
19. Le DT, Durham JN, Smith KN, *et al*. Mismatch repair deficiency predicts response of solid tumors to PD-1 blockade. *Science* 2017; **357:** 409–413.
20. Bach DH, Zhang W, Sood AK. Chromosomal instability in tumor initiation and development. *Cancer Res* 2019; **79:** 3995–4002.
21. Baretti M, Le DT. DNA mismatch repair in cancer. *Pharmacol Ther* 2018; **189:** 45–62.
22. Bonneville R, Krook MA, Kautto EA, *et al*. Landscape of microsatellite instability across 39 cancer types. *JCO Precis Oncol* 2017; **2017:** PO.17.00073.
23. Marabelle A, Fakih M, Lopez J, *et al*. Association of tumour mutational burden with outcomes in patients with advanced solid tumours treated with pembrolizumab: prospective biomarker analysis of the multicohort, open-label, phase 2 KEYNOTE-158 study. *Lancet Oncol* 2020; **21:** 1353–1365.
24. Kim JY, Kim WG, Kwon CH, *et al*. Differences in immune contextures among different molecular subtypes of gastric cancer and their prognostic impact. *Gastric Cancer* 2019; **22:** 1164–1175.
25. Hendry S, Salgado R, Gevaert T, *et al*. Assessing tumor-infiltrating lymphocytes in solid tumors: a practical review for pathologists and proposal for a standardized method from the international immunooncology biomarkers working group: part 1: assessing the host immune response, TILs in invasive breast carcinoma and ductal carcinoma in situ, metastatic tumor deposits and areas for further research. *Adv Anat Pathol* 2017; **24:** 235–251.
26. Herrington CS, Poulsom R, Coates PJ. Recent advances in pathology: the 2020 annual review issue of the journal of pathology. *J Pathol* 2020; **250:** 475–479.
27. García-Corbacho J, Indacochea A, González Navarro AE, *et al*. Determinants of activity and efficacy of anti-PD1/PD-L1 therapy in patients with advanced solid tumors recruited in a clinical trials unit: a longitudinal prospective biomarker-based study. *Cancer Immunol Immunother* 2023; **72:** 1709–1723.
28. Moreira A, Masliah-Planchon J, Callens C, *et al*. Efficacy of molecularly targeted agents given in the randomised trial SHIVA01 according to the ESMO scale for clinical actionability of molecular targets. *Eur J Cancer.* 2019; **121:** 202–209.
29. Le Tourneau C, Delord J-P, Gonçalves A, *et al*. Molecularly targeted therapy based on tumour molecular profiling versus conventional therapy for advanced cancer (SHIVA): a multicentre, open-label, proof-of-concept, randomised, controlled phase 2 trial. *Lancet Oncol* 2015; **16:** 1324–1334.
30. Salgado R, Denkert C, Demaria S, *et al*. The evaluation of tumor-infiltrating lymphocytes (TILs) in breast cancer: recommendations by an international TILs working group 2014. *Ann Oncol* 2015; **26:** 259–271.
31. Burtness B, Harrington KJ, Greil R, *et al*. Pembrolizumab alone or with chemotherapy versus cetuximab with chemotherapy for recurrent or metastatic squamous cell carcinoma of the head and neck (KEYNOTE-048): a randomised, open-label, phase 3 study. *Lancet* 2019; **394:** 1915–1928.
32. Gonzalez-Ericsson PI, Stovgaard ES, Sua LF, *et al*. The path to a better biomarker: application of a risk management framework for the implementation of PD-L1 and TILs as immuno-oncology biomarkers in breast cancer clinical trials and daily practice. *J Pathol* 2020; **250:** 667–684.
33. Mok TSK, Wu Y-L, Kudaba I, *et al*. Pembrolizumab versus chemotherapy for previously untreated, PD-L1-expressing, locally advanced or metastatic non-small-cell lung cancer (KEYNOTE-042): a randomised, open-label, controlled, phase 3 trial. *Lancet* 2019; **393:** 1819–1830.
34. Zeeshan R, Mutahir Z. Cancer metastasis - tricks of the trade. *Bosn J Basic Med Sci* 2017; **17:** 172–182.
35. Remark R, Alifano M, Cremer I, *et al*. Characteristics and clinical impacts of the immune environments in colorectal and renal cell carcinoma lung metastases: influence of tumor origin. *Clin Cancer Res* 2013; **19:** 4079–4091.
36. Loi S, Salgado R, Schmid P, *et al*. Association between biomarkers and clinical outcomes of pembrolizumab monotherapy in patients with metastatic triple-negative breast cancer: KEYNOTE-086 exploratory analysis. *JCO Precis Oncol.* 2023; **7:** e2200317.
37. von Hardenberg J, Hartmann S, Nitschke K, *et al*. Programmed death ligand 1 (PD-L1) status and tumor-infiltrating lymphocytes in hot spots of primary and liver metastases in prostate cancer with neuroendocrine differentiation. *Clin Genitourin Cancer* 2019; **17:** 145–153.e5.
38. Vétizou M, Pitt JM, Daillère R, *et al*. Anticancer immunotherapy by CTLA-4 blockade relies on the gut microbiota. *Science* 2015; **350:** 1079–1084.
39. Sivan A, Corrales L, Hubert N, *et al*. Commensal difidobacterium promotes antitumor immunity and facilitates anti–PD-L1 efficacy. *Science* 2015; **350:** 1084–1089.
40. Cortes J, Cescon DW, Rugo HS, *et al*. Pembrolizumab plus chemotherapy versus placebo plus chemotherapy for previously untreated locally recurrent inoperable or metastatic triple-negative breast cancer (KEYNOTE-355): a randomised, placebo-controlled, double-blind, phase 3 clinical trial. *Lancet* 2020; **396:** 1817–1828.
41. Ullah A, Pulliam S, Karki NR, *et al*. PD-L1 over-expression varies in different subtypes of lung cancer: will this affect future therapies? *Clin Pract* 2022; **12:** 653–671.
42. Qi Y, Zhang L, Wang Z, *et al*. Efficacy and safety of anti-PD-1/ PD-L1 monotherapy for metastatic breast cancer: clinical evidence. *Front Pharmacol* 2021; **12:** 653521.
43. Parsa AT, Waldron JS, Panner A, *et al*. Loss of tumor suppressor PTEN function increases B7-H1 expression and immunoresistance in glioma. *Nat Med* 2007; **13:** 84–88.
44. Song M, Chen D, Lu B, *et al*. PTEN loss increases PD-L1 protein expression and affects the correlation between PD-L1 expression and clinical parameters in colorectal cancer. *PLoS One* 2013; **8:** e65821.
45. Dong H, Strome SE, Salomao DR, *et al*. Tumor-associated B7-H1 promotes T-cell apoptosis: a potential mechanism of immune evasion. *Nat Med* 2002; **8:** 793–800.
46. Li Y, Li F, Jiang F, *et al*. A mini-review for cancer immunotherapy: molecular understanding of PD-1/PD-L1 pathway & translational blockade of immune checkpoints. *Int J Mol Sci* 2016; **17:** 1151.
47. Pardoll DM. The blockade of immune checkpoints in cancer immunotherapy. *Nat Rev Cancer* 2012; **12:** 252–264.
48. Wang HB, Yao H, Li CS, *et al*. Rise of PD-L1 expression during metastasis of colorectal cancer: implications for immunotherapy. *J Dig Dis* 2017; **18:** 574–581.
49. Hong L, Negrao MV, Dibaj SS, *et al*. Programmed death-ligand 1 heterogeneity and its impact on benefit from immune checkpoint inhibitors in NSCLC. *J Thorac Oncol.* 2020; **15:** 1449–1459.
50. Engerud H, Berg HF, Myrvold M, *et al*. High degree of heterogeneity of PD-L1 and PD-1 from primary to metastatic endometrial cancer. *Gynecol Oncol* 2020; **157:** 260–267.

51. Li M, Li A, Zhou S, *et al*. Heterogeneity of PD-L1 expression in primary tumors and paired lymph node metastases of triple negative breast cancer. *BMC Cancer* 2018; **18:** 4.

52. Salgado R, Bellizzi AM, Rimm D, *et al*. How current assay approval policies are leading to unintended imprecision medicine. *Lancet Oncol* 2020; **21:** 1399–1401.

SUPPLEMENTARY MATERIAL ONLINE

Supplementary materials and methods

Figure S1. Sample analysis workflow

Figure S2. Biopsies from metastases by metastatic biopsy location

Figure S3. Distribution of PD-L1 expression (CPS) in metastases according to (A) organ of origin, (B) histological type, and (C) metastatic biopsy site

Figure S4. Distribution of PD-L1 expression (TPS) in metastases according to (A) organ of origin, (B) histological type, and (C) metastatic biopsy site

Figure S5. Distribution of PD-L1 expression (IC) in metastases according to (A) organ of origin, (B) histological type, and (C) metastatic biopsy site

Figure S6. Distribution of PD-L1 expression (CPS) in matched primary tumors and metastases according to (A) organ of origin, (B) histological type, and (C) metastatic biopsy site

Figure S7. Distribution of PD-L1 expression (CPS) in matched primary tumors and metastases according to (A) organ of origin, (B) histological type, and (C) metastatic biopsy site

Figure S8. Distribution of PD-L1 expression (TPS) in matched primary tumors and metastases according to (A) organ of origin, (B) histological type, and (C) metastatic biopsy site

Figure S9. Distribution of PD-L1 expression (TPS) in matched primary tumors and metastases according to (A) organ of origin, (B) histological type, and (C) metastatic biopsy site

Figure S10. Distribution of PD-L1 expression (IC) in matched primary tumors and metastases according to (A) organ of origin, (B) histological type, and (C) metastatic biopsy site

Figure S11. Overall survival according to (A) organ of origin, (B) histological type, and (C) metastatic biopsy site

Figure S12. Overall survival according to TIL proportion

Figure S13. Overall survival according to TIL proportion and organ of origin

Figure S14. Overall survival according to TIL proportion and histological subtype

Figure S15. Overall survival according to TIL proportion and metastatic biopsy site

Table S1. TIL proportion and PD-L1 expression in metastases

Table S2. PD-L1 expression in metastases using three scores (CPS, TPS, and ICS)

Table S3. PD-L1 expression in matched primary and metastatic tumor samples using the CPS, TPS, and ICS

Table S4. TIL proportion and PD-L1 expression in matched primary tumors and metastases